

# CARBON NANOHORNS – BASED NANOCOMPOSITES AS SENSING LAYERS FOR ROOM TEMPERATURE RESISTIVE OXYGEN SENSING: PRELIMINARY RESULTS

BOGDAN-CATALIN SERBAN<sup>1,2</sup>, OCTAVIAN BUIU<sup>1</sup>, NICULAE DUMBRAVESCU<sup>1</sup>,  
MIHAI BREZEANU<sup>3</sup>, CORNEL COBIANU<sup>4</sup>, CRISTINA PACHIU<sup>1</sup>,  
OANA BRANCOVEANU<sup>1</sup>, MARIUS BUMBAC<sup>5,6</sup>, CRISTINA MIHAELA NICOLESCU<sup>6</sup>,  
CRISTIANA RADULESCU<sup>5,6</sup>

Manuscript received: 02.10.2023; Accepted paper: 15.01.2024;

Published online: 30.03.2024.

**Abstract.** This paper presents the oxygen sensing response of a resistive sensor employing sensing layers based on a binary matrix nanocomposite such as carbon nanohorns/polyvinylpyrrolidone and oxidized carbon nanohorns/polyvinylpyrrolidone, both at 9/1 w/w/ mass ratio. The sensing structure comprises a silicon substrate, a SiO<sub>2</sub> layer, and interdigitated transducers (IDT) electrodes, on which the sensing layer is deposited via the drop-casting method. The thin film's morphology and composition are examined through scanning electron microscopy (SEM) and RAMAN spectroscopy. The oxygen sensing capability of each carbon nanohorns composite-based sensing layer was analyzed by applying a current between the two electrodes and measuring the voltage difference when varying the O<sub>2</sub> from 0% to 100% in dry nitrogen. Experiments reveal that in the case of pristine carbon nanohorns / PVP matrix nanocomposite, the resistance increases. In contrast, in the case of oxidized carbon nanohorns, the resistance of the sensitive layer decreases with increasing oxygen concentration. The results are explained by considering the differences from structural and electrical points of view between the two types of nanocarbonic materials. Moreover, previous resistive RH sensing measurements in humid air and humid nitrogen using oxidized carbon nanohorns as sensing elements proved helpful in better understanding and discriminating between the chemisorption/physisorption of oxygen molecules at carboxyl functional sites and graphitic carbon sites.

**Keywords:** oxidized carbon nanohorns; polyvinylpyrrolidone; p-type semiconductor.

## 1. INTRODUCTION

Besides carbon nanotubes [1], graphene [2], graphene oxide [3], reduced graphene oxide [4], nanodiamond [5] fullerenes [6], quantum dots [7], carbon nano onions [8], carbon nanohorns and their derivatives [9] have also emerged as interesting nanocarbonic structures.

<sup>1</sup> National Institute for Research and Development in Microtechnologies, IMT-Bucharest, 077190 Voluntari, Romania. E-mail: [bogdan.serban@imt.ro](mailto:bogdan.serban@imt.ro).

<sup>2</sup> Zentiva Romania S.A, 032266 Bucharest, Romania.

<sup>3</sup> National University of Science and Technology Politehnica of Bucharest, Faculty of Electronics, Telecommunications and IT, 060042 Bucharest, Romania.

<sup>4</sup> Academy of Romanian Scientists, 050044 Bucharest, Romania.

<sup>5</sup> Valahia University of Targoviste, Faculty of Sciences and Arts, Department of Sciences and Advanced Technologies, 130004 Targoviste, Romania.

<sup>6</sup> Valahia University of Targoviste, Institute of Multidisciplinary Research for Science Technology, 130004 Targoviste, Romania.

Single-walled carbon nanohorns (SWCNHs, Fig.1a), consisting of closed cages of  $sp^2$ -bonded carbon atoms, typically 2–5 nm in diameter and 40–50 nm in length, were first reported by Iijima in 1998 [10]. These structures exhibit several outstanding intrinsic characteristics, such as facile synthesis procedure, high dispersibility, high mechanical strength, good electrical and thermal conductivity, high specific surface area, large porosity, and versatile approaches for covalent and noncovalent functionalization [11-13].

Therefore, potential applications of SWCNHs include supercapacitors [14], gas storage [15], photovoltaics [16], drugs delivery system carriers [17], fuel and biofuel cells [18], lubricants [19], refrigerators [20], electrochemical sensor [21] and so forth. In the last years, carbon nanohorns (pristine and oxidated) and their nanocomposites/nanohybrids have been widely used as sensing films in resistive detection of relative humidity [22-34] and some gases such as ethanol [35-37], ozone [38], ammonia [39], hydrogen sulfide [40].

On the other hand, measuring the oxygen concentration is essential in several fields, such as industrial processes monitoring (steel and cement industries, production of carbonated soda), automotive (control of air-fuel mixture in combustion engine, emission monitoring), medicine (i.e., anesthesia monitors), food packaging (monitoring oxygen concentration in blanket gas for coffee, milk, and other powders for product quality), environmental and marine monitoring (limnology and waste management) [41-45]. Various technological approaches have been developed for oxygen monitoring, including reflectometry [46,47], fluorescence quenching [48], infrared and Raman spectroscopy [49], interferometry [50], and electrochemistry [51]. More widely, resistive sensors are an inexpensive alternative for detecting oxygen molecules [52, 53]. Among the materials most used as sensing layers in the design of resistive oxygen sensors, we can enumerate metal oxide semiconductors [54, 55] and carbonic materials [56, 57].

This paper presents the preliminary results concerning the response of a resistive oxygen sensor that uses a sensing layer based on CNH/PVP and CNHox/PVP for both matrix nanocomposites w/w/w/w ratios of the constituents are 9/1. Differences between molecular structures of nanocarbonic materials and subtle differences regarding the interaction with oxygen molecules are responsible for the obtained results.

## 2. MATERIALS AND METHODS

### 2.1. MATERIALS

Both necessary nanocarbon materials for synthesizing carbon nanohorns–based matrix nanocomposite used in chemo-resistive oxygen sensing experiments were purchased from Sigma Aldrich (Redox Lab Supplies Com, Bucharest, Romania). Pristine carbon nanohorns (abbreviated as CNHs-Fig. 1a) are characterized by a specific surface area of around 400  $m^2/g$  (according to Brunauer-Emmett-Teller surface area analysis) and diameters between 2 nm and 5 nm.

CNHox (Fig. 1b) are characterized by lengths between 40 nm and 50 nm, diameters between 2 nm to 5 nm, and a specific surface area of around 1,300-1,400  $m^2/g$  (according to Brunauer-Emmett-Teller surface area analysis). Both nanocarbonic materials contain 10% graphite as the main impurity and have no metal contamination.

Polyvinylpyrrolidone (abbreviated as PVP, depicted in Fig.1c, with an average mol wt 40,000), isopropanol (70% w/w in water), and dimethylformamide (abbreviated as DMF) were also purchased from Sigma-Aldrich. All chemicals were used without further purification.

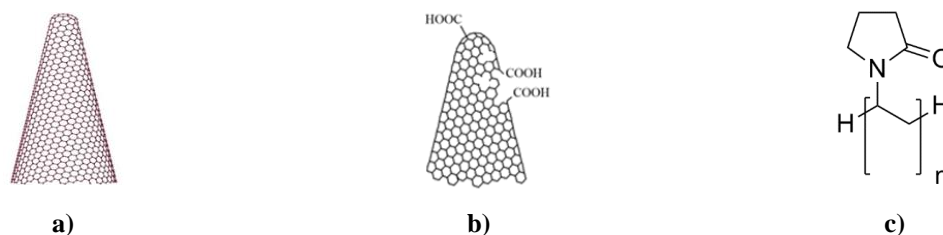


**Figure 1. Structure of: a) carbon nanohorns; b) oxidated carbon nanohorns, and c) PVP.**

## 2.2. METHODS

The homogenization of the prepared dispersions was performed using a mild sonication bath (FS20D Fisher Scientific, Dreieich, Germany) at 42 kHz (output power 70 W). This procedure ensured a relatively uniform dispersion of the CNHs, CNHox, in the PVP matrix. The Raman spectra were collected at room temperature with a Witec Raman spectrometer (Alpha-SNOM 300 S, WiTec. GmbH, Ulm, Germany) using 532 nm as an excitation. The 532-nm diode-pumped solid-state laser has a maximum power of 145 mW. The incident laser beam with a spot size of about 1.0  $\mu\text{m}$  was focused onto the sample with a 100  $\times$  long-working distance microscope objective. The Raman spectra were recorded using a 20 s exposure time; the scattered light was collected by the same objective in back-scattering geometry with 600 grooves/mm grating. The Raman system was calibrated using the 512  $\text{cm}^{-1}$  Raman line of a silicon substrate, which corresponds to the longitudinal optical-transverse optical (LO-TO) phonon. The spectrometer scanning data collection and processing were carried out by a dedicated computer using WiTec Project Five software (WiTec Project Five 5.1, WiTec. GmbH, Ulm, Germany).

Surface topography of the sensing layers based on quaternary hybrid nanocomposite was investigated by scanning electron microscopy (SEM). For surface inspection, a field emission gun scanning electron microscope / FEG-SEM-Nova NanoSEM 630 (Thermo Scientific, Waltham, MA, USA) (FEI), with superior low voltage resolution and high surface sensitivity imaging, was employed.

The synthesis of the solid-state sensing films based on matrix nanocomposite CNHs-PVP = 9:1 (w/w) and CNHox -PVP = 9:1(w/w) is described below:

- The polyvinylpyrrolidone solution is prepared by dissolving 1 mg of polymer in 10 mL of dimethylformamide under magnetic stirring for two hours at room temperature.
- 9 mg of nanocarbon material (CNHs or CNHox) were dispersed in the previously prepared and stirred in an ultrasonic bath for six hours at room temperature.
- The obtained dispersion is deposited by the "drop casting" method using a Si/SiO<sub>2</sub> substrate with linear electrodes (after masking the contact area beforehand).
- The sensitive layer obtained is subjected to a heat treatment at 100°C, for 90 minutes, in a vacuum.

The sensing device consisted of a metallic interdigitated (IDT) dual-comb structure fabricated on a Si substrate (470  $\mu\text{m}$  thickness), covered by a SiO<sub>2</sub> layer (1  $\mu\text{m}$  thickness) (Fig. 2). The metal stripes of IDT were comprised of chromium (10 nm thickness) and gold (100 nm thickness). The digits' width and spacing were equal to 10 microns, with a 0.6 mm separation between the digits and the bus bar.

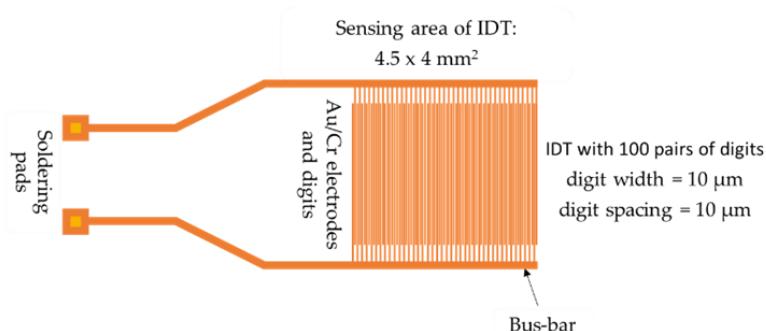


Figure 2. Sensing device architecture

Tests for the capability of the as-prepared nanocomposites CNHs/PVP and CNHox/PVP to monitor the oxygen concentration variations were performed in the experimental setup shown in Fig. 3. Thus, the sensing layer was included in a device-under-testing (DUT) and exposed to different oxygen concentrations created in the testing environment. Measurements were performed in nitrogen at room temperature, to which pure, anhydrous oxygen was added. Experiments consisted of applying an electrical current between the electrodes and measuring the resulting voltage for different values of oxygen concentrations. A mass flow controller was used to control the gas inlets in the testing chamber.

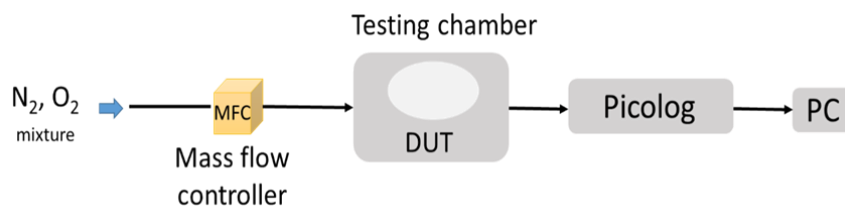


Figure 3. Experimental setup employed for O<sub>2</sub> resistive measurement

### 3. RESULTS AND DISCUSSION

#### 3.1. RESULTS

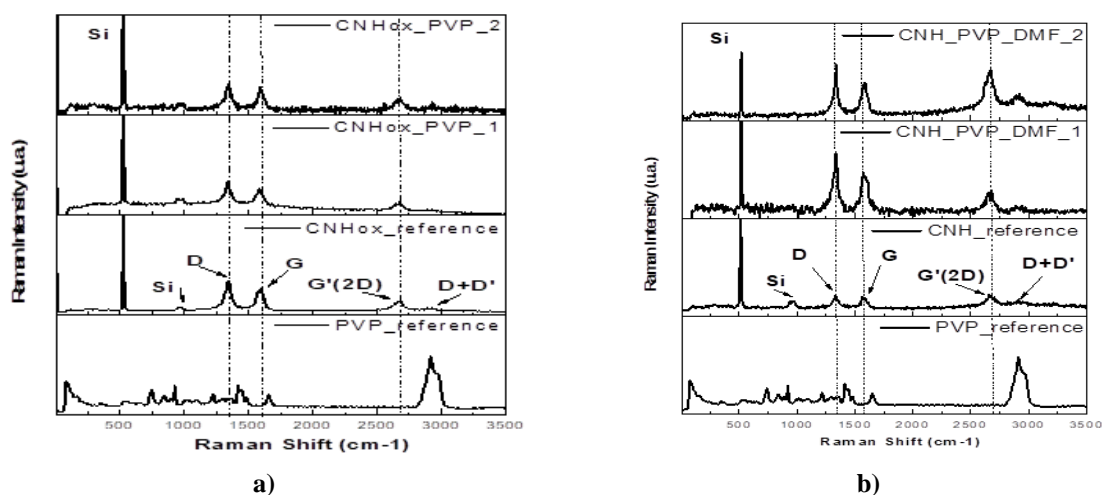


Figure 4. Raman spectra of solid-state films deposited on the silicon substrate for: a) CNHox/PVP 9/1 (w/w), and b) CNHs/PVP 9/1 (w/w).

The recorded Raman spectrum (Fig. 4) exhibits the typical D ( $\sim 1337.5 \text{ cm}^{-1}$ ), G ( $\sim 1587.4 \text{ cm}^{-1}$ ), and second-order bands of 2D and D+D' band localized at  $2667.5$  and  $2924.9 \text{ cm}^{-1}$  which are typical for oxidated carbon nanohorns. The very high intensity of the peak located at  $\cong 520 \text{ cm}^{-1}$  is associated with the silicon substrate [58]. Moreover, the typical peaks assigned to PVP ( $858, 1437, 1669, 2937, \text{ and } 2994 \text{ cm}^{-1}$ ) [59] are overlapped with the peaks of CNHox. Some of the small Raman shifts of the peaks associated with oxidized carbon nanohorn materials are a consequence of hydrogen bonds with polyvinylpyrrolidone.

The Raman spectra of solid-state films of CNHs/PVP 9/1 (mass ratio) deposited on the silicon substrate are quasi-similar to the previously discussed Raman spectra. The small differences can be interpreted as structural differences between carbon nanohorns and oxidized carbon nanohorns [33-37].

The surface morphology of the deposited films was relatively homogenous in all cases (Figs. 5 and 6). The hydrogen bond between CNHox and PVP and the film-forming properties of PVP are two factors that could explain these results.

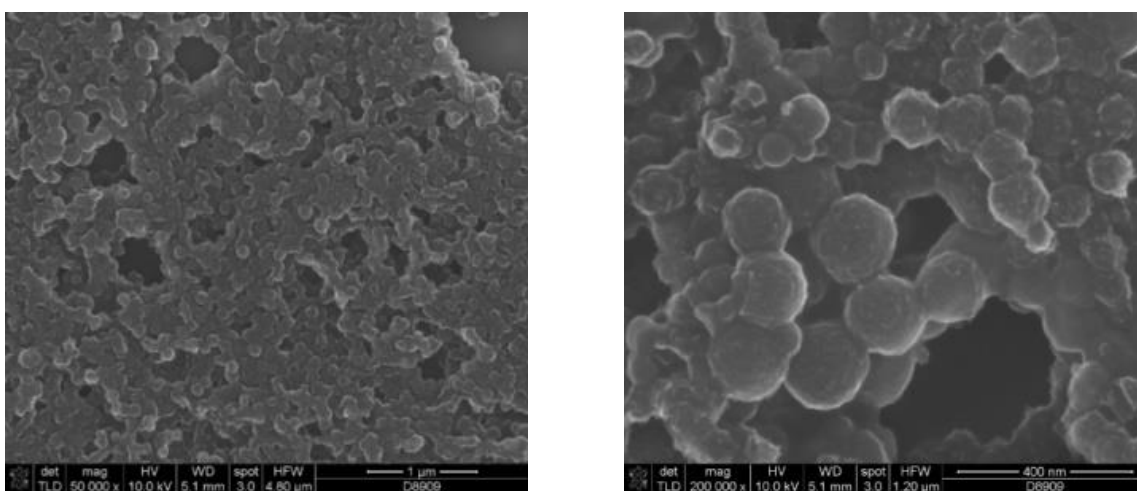


Figure 5. Scanning electron micrographs of the CNHs/PVP (9/1, w/w): (a)  $\times 50,000$  magnification; (b)  $\times 200,000$  magnification.

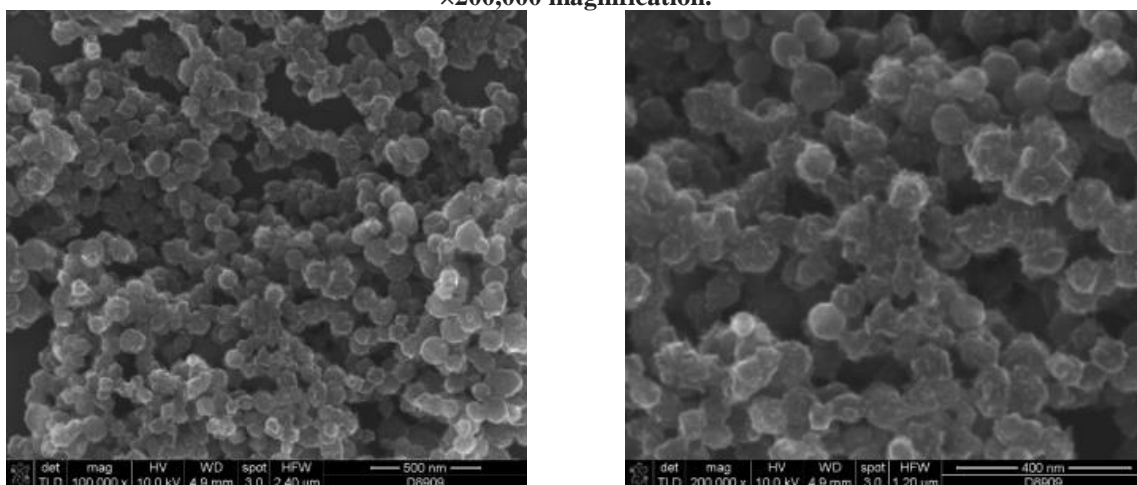


Figure 6. Scanning electron micrographs of the CNHox/PVP (9/1, w/w): (a)  $\times 100,000$  magnification; (b)  $\times 200,000$  magnification

It appears that the surface topography of these sensing layers presents a uniform surface without islands, showing good dispersion of carbonaceous material in the polymeric matrix. At first glance, regions are uniform with good dispersion of the nanomaterial. The nanoscale images reveal the existence of a wide particle size distribution, starting from about 10-30 nm to 100 nm.

The behavior of the manufactured sensors is presented in Figs. 7 and 8. The mass ratio of nanocarbonic material/polymer was 9:1 in both matrix nanocomposites. This ratio was chosen to exploit the forming properties of PVP and to avoid the disadvantages generated by the low permeability of oxygen gas. Conducted experiments show interesting results. In the case of pristine carbon nanohorns/PVP matrix nanocomposite the resistance increases (Fig. 7), while in the case of oxidized carbon nanohorns, the resistance of the sensitive layer decreases with increasing oxygen concentration (Fig. 8).

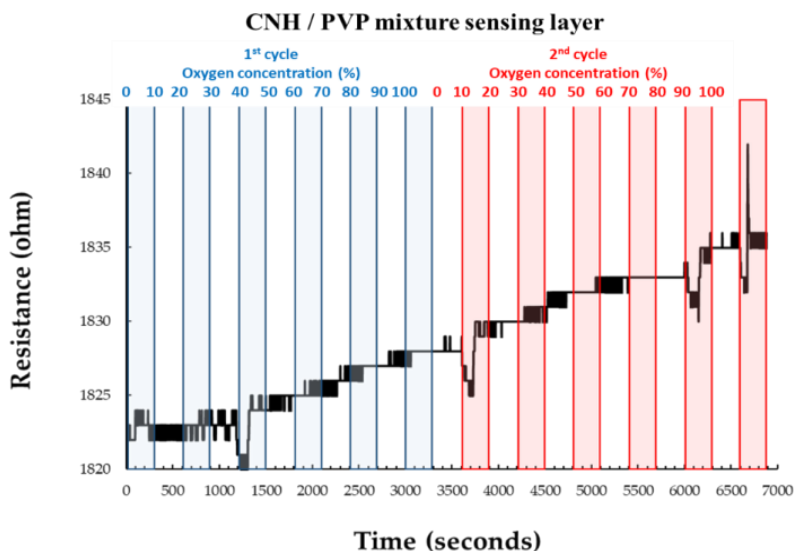


Figure 7. The response of CNH/PVP sensing layer-based sensor as a function of time for two measurement cycles when oxygen concentration was increased in ten steps from 0% O<sub>2</sub> to 100% O<sub>2</sub>

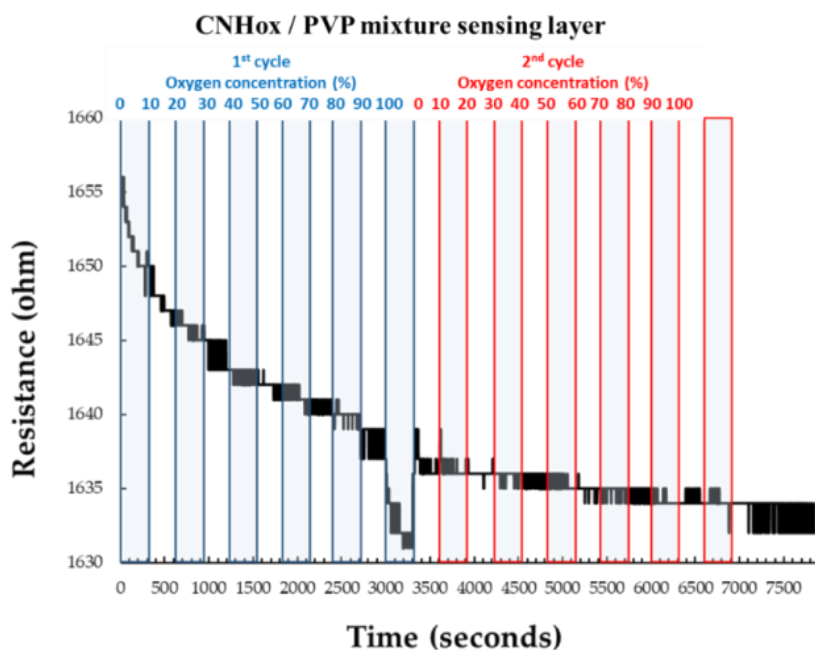


Figure 8. The response of CNHox/PVP sensing layer-based sensor as a function of time for two measurement cycles when oxygen concentration was increased in ten steps from 0% O<sub>2</sub> to 100% O<sub>2</sub>

## 4. DISCUSSIONS

The oxygen molecule is a typical example of an electron acceptor, whose electron affinity is 0.4-0.5 eV [60]. It is accepted that oxidized carbon nanohorns are p-type semiconductors. Thus, the chemisorbed oxygen molecules accept electrons from the CNHox, new holes are created, thus decreasing the electrical resistance (electrical conductivity increases).

The conclusions of the performed experiments are in agreement with the theoretical predictions. In the case of pristine carbon nanohorns, the situation is reversed. Several literature studies reveal that pristine carbon nanohorns are n-type semiconductors [60]. This conclusion is based on a result of the change in the electrical resistance of pristine carbon nanohorns-based sensing film upon exposure to carbon dioxide, a typical electron donor. The increase in the conductivity of the film (by accepting electrons from CO<sub>2</sub>) suggests for simple carbon nanohorns a typical n-type semiconductor behavior. This hypothesis is consistent with the experimental results in the case of oxygen monitoring. Supposing an n-type semiconductor, exposure to oxygen (electron acceptor) leads to a decrease of the concentration of electrons from the conduction band and therefore to a decrease of electrical conductivity, respectively to an increase in resistance.

However, a closer examination of the CNHox structure (Fig. 1) raises the following question: does the chemisorption/ physisorption of oxygen molecules take place at (a) carboxyl functional sites or (b) graphitic carbon sites, or (c) in both positions? An indirect argument that confirms that chemisorption/physisorption of oxygen molecules *can* take place even at carboxyl functional sites is the higher sensitivity of CNHox when varying RH from 10% to 90%, in humid air in comparison with humid nitrogen (21 mΩ/RH unit compared to 9.1 mΩ/RH unit, see the Figs. 9 and 10) [23]:

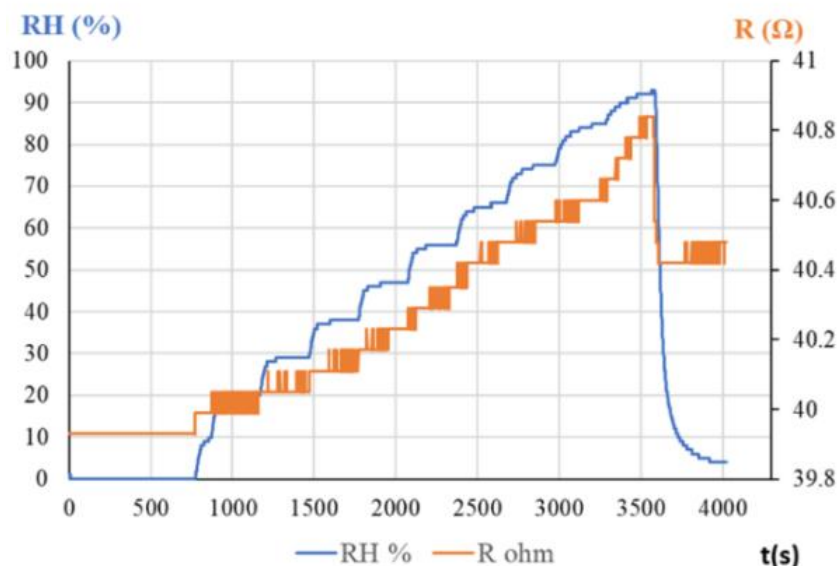


**Figure 9.** The RH response of the CNHox-based sensor in humid nitrogen (red curve) vs. the RH response of the reference Sensirion RH sensor (blue curve)

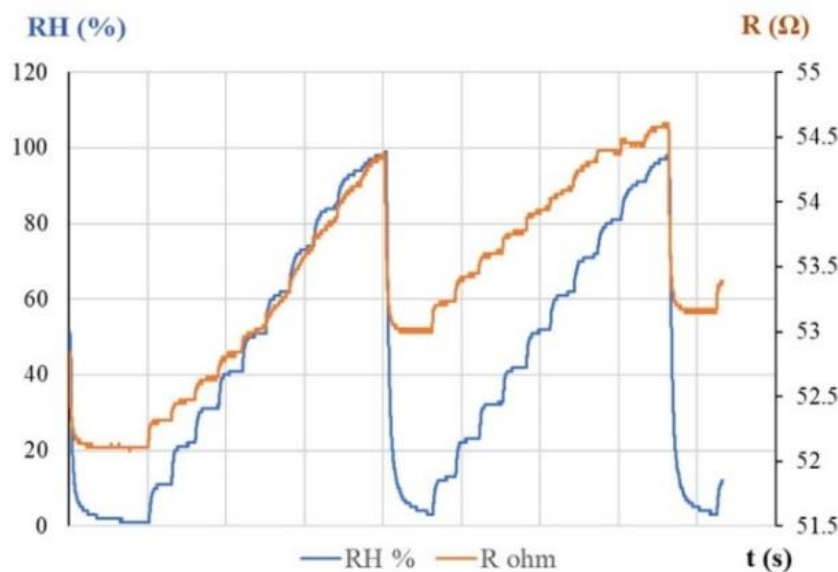


**Figure 10.** The RH response of the oxidized CNHox-based sensor in humid air (red curve) vs. the RH response of the reference Sensirion RH sensor (blue curve)

The results can be explained if we consider that most oxygen molecules present in the humid air are mainly absorbed into the polar carboxyl groups on the CNHox. The oxygen molecules are polarizable and can form hydrogen bonding with the hydroxyl moiety in the carboxyl group. Thus, the electron-withdrawing effect of the carboxyl group is, partly, suppressed. Thus, hole carrier concentration on the CNHox decreases, yielding a minor overall increase in resistance for the carbonaceous sensing film, even though oxygen molecules chemisorption/ physisorption graphitic carbon sites could yield an antithetical electrical response, according to the previous experiments.

The presence of carboxylic groups onto the molecular architecture CNHox seems to be a key structural feature. Therefore, we can say that in the case of the detection of oxygen in the presence of dry nitrogen chemisorption/ physisorption of oxygen molecules takes place both at carboxyl functional and graphitic carbon sites, positioning on the last site being prevalent.

## 5. CONCLUSIONS

This paper presents the oxygen sensing response of a resistive sensor employing sensing layers based on a binary matrix nanocomposite such as carbon nanohorns/polyvinylpyrrolidone and oxidized carbon nanohorns/polyvinylpyrrolidone, both at 9/1 w/w mass ratios. Experiments reveal that in the case of pristine carbon nanohorns/PVP matrix nanocomposite the resistance increases while in the case of oxidized carbon nanohorns, the resistance of the sensitive layer decreases with increasing oxygen concentration.

The interpretation of results considers the electron acceptor character of oxygen molecules, the *n*-type semiconductor nature of pristine carbon nanohorns, *p*-type semiconductor behavior of oxidized carbon nanohorns. Moreover, the chemisorption/ physisorption of oxygen molecules at carboxyl functional sites and graphitic carbon sites plays a cardinal role in the overall response of the sensing film towards oxygen molecules.



Previous resistive RH sensing measurements in humid air and humid nitrogen using oxidized carbon nanohorns as sensing elements were useful to take into account the chemisorption/physorption of oxygen molecules at the carboxyl functional group. However, based on the electrical overall response we conclude that chemisorption/physorption of gas molecules at graphitic carbon sites is prevalent.

**Acknowledgments:** *The authors would like to acknowledge the financial support provided by the Romanian Ministry of Education and Research via the “MICRO-NANO-SIS PLUS” Nucleu program, grant number PN 19 16, and contract no 364PED – 23.10.2020, CASTOL, financed by The Executive Agency for Higher Education, Research, Development, and Innovation Funding (UEFISCDI).*

## REFERENCES

- [1] Dai, H., *Surface Science*, **500**(1-3), 218, 2002.
- [2] Geim, A.K., *Science*, **324**(5934), 1530, 2009.
- [3] Marcano, D.C., Kosynkin, D.V., Berlin, J.M., Sinitskii, A., Sun, Z., Slesarev, A., Alemany, L.B., Lu, W., Tour, J.M., *ACS Nano*, **4**(8), 4806, 2010.
- [4] Tarcan, R., Todor-Boer, O., Petrovai, I., Leordean, C., Astilean, S., Botiz, I., *Journal of Materials Chemistry C*, **8**(4), 1198, 2020.
- [5] Schrand, A.M., Hens, S.A.C., Shenderova, O.A., *Critical Reviews in Solid State and Materials Sciences*, **34**(1-2), 18, 2009.
- [6] Taylor, R., Walton, D.R. *Nature*, **363**(6431), 685, 1993.
- [7] Lim, S.Y., Shen, W., Gao, Z. *Chemical Society Reviews*, **44**(1), 362, 2015.
- [8] Bartelmess, J., Giordani, S., **5**(1), 1980, 2014.
- [9] Zhu, S., Xu, G. *Nanoscale*, **2**(12), 2538, 2010.
- [10] Iijima, S., Yudasaka, M., Yamada, R., Bandow, S., Suenaga, K., Kokai, F., Takahashi, K., *Chemical Physics Letters*, **309**, 165, 1999.
- [11] Berber, S., Kwon, Y.K., Tomanek, D., *Physical Review B*, **62**(4), R2291, 2000.
- [12] Pagona, G., Mountrichas, G., Rotas, G., Karousis, N., Pispas, S., Tagmatarchis, N., *International Journal of Nanotechnology*, **6**(1-2), 176, 2009.
- [13] Zieleniewska, A., Lodermeier, F., Prato, M., Rumbles, G., Guldi, D.M., Blackburn, J.L., *Journal of Materials Chemistry C*, **10**(15), 5783, 2022.
- [14] Izadi-Najafabadi, A., Yamada, T., Futaba, D.N., Yudasaka, M., Takagi, H., Hatori, H., Iijima, S., Hata, K., *ACS Nano*, **5**(2), 811, 2011.
- [15] Bekyarova, E., Murata, K., Yudasaka, M., Kasuya, D., Iijima, S., Tanaka, H., Kahoh, H., Kaneko, K., *Journal of Physical Chemistry B*, **107**(20), 4681, 2003.
- [16] Lodermeier, F., Costa, R.D., Guldi, D.M., *Advanced Energy Materials*, **7**(10), 1601883, 2017.
- [17] Ajima, K., Yudasaka, M., Murakami, T., Maigne, A., Shiba, K., Iijima, S., *Molecular Pharmaceutics*, **2**(6), 475, 2005.
- [18] Wen, D., Deng, L., Zhou, M., Guo, S., Shang, L., Xu, G., Dong, S., *Biosensors and Bioelectronics*, **25**(6), 1544, 2010.
- [19] Kobayashi, K., Hironaka, S., Tanaka, A., Umeda, K., Iijima, S., Yudasaka, M., Kasuya, D., Suzuki, M., *Journal Japan Petroleum Institute*, **48**(3), 121, 2005.

- [20] Alawi, O. A., Sidik, N.A.C., *International Communications in Heat and Mass Transfer*, **68**, 91, 2015.
- [21] Zhu, G., Sun, H., Zou, B., Liu, Z., Sun, N., Yi, Y., Wong, K.Y., *Biosensors and Bioelectronics*, **106**, 136, 2018.
- [22] Selvam, K.P., Nakagawa, T., Marui, T., Inoue, H., Nishikawa, T., Hayashi, Y., *Materials Research Express*, **7**(5), 056402, 2020.
- [23] Serban, B.C., Buiu, O., Dumbravescu, N., Cobianu, C., Avramescu, V., Brezeanu, M., Bumbac, M., Nicolescu, C.M., *Acta Chimica Slovenica*, **67**(2), 469, 2020.
- [24] Şerban, B.C., Buiu, O., Dumbravescu, N., Avramescu, V., Brezeanu, M., Marinescu, M. R., Bumbac, M., Nicolescu, C., EMERGEMAT, *5<sup>th</sup> International Conference, Emerging technologies in Engineering Materials, Bucharest, Romania*, Carbon nanohorns-based matrix nanocomposite for relative humidity sensor, Book of abstract, p. 90, 2022.
- [25] Serban, B.C., Buiu, O., Dumbravescu, N., Cobianu, C., Avramescu, V., Brezeanu, M., Bumbac, M., Pachiu, C., Nicolescu, C.M., *Analytical Letters*, **54**(3), 527, 2021.
- [26] Şerban, B.C., Buiu, O., Cobianu, C., Avramescu, V., Dumbravescu, N., Brezeanu, M., Bumbac, M., Nicolescu, C.M., Marinescu, R., *Multidisciplinary Digital Publishing Institute Proceedings*, **29**(1), 114, 2019.
- [27] Serban, B.C., Cobianu, C., Buiu, O., Bumbac, M., Dumbravescu, N., Avramescu, V., Nicolescu, C. M., Brezeanu, M., Pachiu, C., Craciun, G., Radulescu, C., *Materials*, **14**(11), 2705, 2021.
- [28] Serban, B.C., Cobianu, C., Buiu, O., Bumbac, M., Dumbravescu, N., Avramescu, V., Nicolescu, C.M., Brezeanu, M., Radulescu, C., Craciun, G., Romanitan, C., *Coatings*, **11**(11), 1307, 2021.
- [29] Serban, B.C., Buiu, O., Bumbac, M., Dumbravescu, N., Avramescu, V., Brezeanu, M., Radulescu, C., Craciun, G., Nicolescu, C.M., Romanitan, C., Comanescu, F., *Coatings*, **11**(9), 1065, 2021.
- [30] Serban, B.C., Buiu, O., Bumbac, M., Marinescu, R., Dumbravescu, N., Avramescu, V., Cobianu, C., Nicolescu, C.M., Brezeanu, M., Radulescu, C., Comanescu, F., *Chemistry Proceedings*, **5**(1), 12, 2021.
- [31] Serban, B.C., Dumbravescu, N., Buiu, O., Bumbac, M., Brezeanu, M., Cobianu, C., Marinescu, R., Pachiu, C., Avramescu, V., Nicolescu, C.M., *Sensor International Semiconductor Conference, CAS 2023, Sinaia, October 11-13, 2023, IEEE event*, Oxidized Carbon Nanohorns/KCl/ PVP Nanohybrid as Sensing Layer for Chemiresistive Humidity Sensor, pp 75, 2023.
- [32] Serban, B.C., Dumbravescu, N., Buiu, O., Bumbac, M., Brezeanu, M., Cobianu, C., Marinescu, R., Pachiu, C., Avramescu, V., Nicolescu, C.M., *International Semiconductor Conference, CAS 2023, Sinaia, October 11-13, 2023, IEEE event*, Ternary Holey Carbon-Based Nanohybrid for Resistive Relative Humidity Sensor, pp 25, 2023.
- [33] Serban, B.C., Cobianu, C., Dumbravescu, N., Buiu, O., Bumbac, M., Nicolescu, C.M., Cobianu, C., Brezeanu, M., Pachiu, C., Serbanescu, M., *Sensors*, **21**(4), 1435, 2021.
- [34] Serban, B.C., Cobianu, C., Dumbravescu, N., Buiu, O., Avramescu, V., Bumbac, M., Nicolescu, C.M., Cobianu, C., Brezeanu, M., *International Semiconductor Conference (CAS)*, Electrical Percolation Threshold In Oxidized Single Wall Carbon Nanohorn-Polyvinylpyrrolidone Nanocomposite: A Possible Application For High Sensitivity Resistive Humidity Sensor, (pp. 239-242). IEEE, 2020.

- [35] Cobianu, C., Serban, B.C., Dumbravescu, N., Buiu, O., Avramescu, V., Pachiu, C., Bita, B., Bumbac, M., Nicolescu, C.M., Cobianu, C., *Nanomaterials*, **10**(12), 2552, 2020.
- [36] Cobianu, C., Serban, B.C., Dumbravescu, N., Buiu, O., Avramescu, V., Bumbac, M., Nicolescu, C.M., Cobianu, C., *International Semiconductor Conference (CAS)*, Room Temperature Chemiresistive Ethanol Detection by Ternary Nanocomposites of Oxidized Single Wall Carbon Nanohorn (ox-SWCNH), pp. 13., 2020.
- [37] Serban, B.C., Dumbravescu, N., Buiu, O., Bumbac, M., Brezeanu, M., Cobianu, C., Marinescu, R., Pachiu, C., Avramescu, V., Nicolescu, C.M., Comanescu, F., *International Semiconductor Conference, CAS 2023, Sinaia, October 11-13, 2023, IEEE event, Proceedings*, Quaternary Oxidized Carbon Nanohorns -Based Nanohybrid as Sensing Layer for Room Temperature Resistive Ethanol Sensing, pp 67, 2023.
- [38] Sano, N., Ohtsuki, F. *Journal of Electrostatics*, **65**(4), 263, 2007.
- [39] Sano, N., Kinugasa, M., Otsuki, F., Suehiro, J., *Advanced Powder Technology*, **18**(4), 455, 2007.
- [40] Zhou, M., Yao, Y., Han, Y., Xie, L., Zhao, X., Barsan, N., Zhu, Z., *Sensors and Actuators B: Chemical*, **354**, 131224, 2022.
- [41] Ramamoorthy, R., Dutta, P.K., Akbar, S.A., *Journal of Materials Science*, **38**, 4271, 2003.
- [42] O'Riordanordan, T.C., Voraberger, H., Kerry, J.P., Papkovsky, D.B., *Analytica Chimica Acta*, **530**(1), 135, 2005.
- [43] Mallik, A., *10<sup>th</sup> Asian control conference (ASCC)*, State feedback based control of air-fuel-ratio using two wide-band oxygen sensors, (pp. 1-6). IEEE, 2015.
- [44] Westenskow, D. R., Jordan, W. S., Jordan, R., Gillmor, S. T., *Anesthesia and Analgesia*, **60**(1), 53, 1981.
- [45] Schwank, J.W., DiBattista, M., *MRS Bulletin*, **24**(6), 44, 1999.
- [46] Eich, S., Schmalzlin, E., Lohmannsroben, H.G., *Sensors*, **13**(6), 7170, 2013.
- [47] Quaranta, M., Borisov, S.M., Klimant, I., *Bioanalytical Reviews*, **4**, 115, 2012.
- [48] Serban, B.C., Costea, S., Buiu, O., Cobianu, C., Diaconu, C. *CAS 2012 International Semiconductor Conference*, Pyrene-1-butyric acid-doped polyaniline for fluorescence quenching-based oxygen sensing, (Vol. 2, pp. 265-268). IEEE, 2012
- [49] Tiwari, V.S., Kalluru, R.R., Yueh, F.Y., Singh, J.P., Cyr, W.S., Khijwania, S.K., *Applied Optics*, **46**(16), 3345, 2007.
- [50] Wang, X.D., Wolfbeis, O.S., *Chemical Society Reviews*, **43**(10), 3666, 2014.
- [51] Cobianu, C., Serban, B., Avramescu, V., Hobbs, B., Pratt, K., Willett, M., *CAS International Semiconductor Conference*, Lead-free galvanic oxygen sensors — A conceptual approach, Vol. 1, pp. 161-164. IEEE., 2012
- [52] Moos, R., Izu, N., Rettig, F., Rei, S., Shin, W., Matsubara, I., *Sensors*, **11**(4), 3439, 2011.
- [53] Rothschild, A., Tuller, H.L., *Resistive Oxygen Sensors (Chapter 6) in Science and Technology of Chemiresistor Gas Sensors*, Nova Science Publishers Hauppauge, NY, pp. 215-256, 2007.
- [54] Stratulat, A., Serban, B.C., de Luca, A., Avramescu, V., Cobianu, C., Brezeanu, M., Buiu, O., Diamandescu, L., Feder, M., Ali, S.Z., Udrea, F., *Sensors*, **15**(7), 17495, 2015.
- [55] Serban, B.C., Brezeanu, M., Cobianu, C., Costea, S., Buiu, O., Stratulat, A., Varachiu, N., *International Semiconductor Conference (CAS)*, Materials selection for gas sensing. An HSAB perspective, (pp. 21-30). IEEE, 2014
- [56] Rajavel, K., Lalitha, M., Radhakrishnan, J.K., Senthilkumar, L., Rajendra Kumar, R.T., *ACS Applied Materials and Interfaces*, **7**(43), 23857, 2015.

- [57] Collins, P.G., Bradley, K., Ishigami, M., Zettl, D.A., *Science*, **287**(5459), 1801, 2000.
- [58] Ajito, K., Sukamto, J.P.H., Nagahara, L.A., Hashimoto, K., Fujishima, A., *Journal of Vacuum Science and Technology A*, **13**, 1234, 1995.
- [59] Jabbarnia, A., Asmatulu, R., *Journal of Materials Science and Technology*, **2**, 43, 2015.
- [60] Urita, K., Seki, S., Utsumi, S., Noguchi, D., Kanoh, H., Tanaka, H., Hattori, Y., Ochiai, Y., Aoki, N., Yudasaka, M., Iijima, S., *Nano Letters*, **6**(7), 1325, 2006.